# Subcooled Forced Convection Film Boiling Drag and Heat Transfer of a Wedge

P. R. Chappidi*
*Los Alamos National Laboratory, Los Alamos, New Mexico 87545*
F. S. Gunnerson†
*University of Central Florida, Orlando, Florida 32816*
and
K. O. Pasamehmetoglu‡
*Los Alamos National Laboratory, Los Alamos, New Mexico 87545*

**Subcooled laminar forced convection film boiling flow on a wedge is analyzed considering the streamwise pressure gradient imposed on the flow and the streamwise buoyancy force acting on the vapor film. A two-phase boundary-layer model is proposed, and the local similarity concept is applied to obtain an approximate solution of the governing equations. For a water-steam system at atmospheric pressure considered within this study, wall skin friction results display a strong dependency on the streamwise buoyancy force driving the vapor film and the external pressure gradient. Adverse streamwise buoyancy force acting on the vapor film, which is the case on the lower surface of a horizontally aligned wedge, may cause vapor flow separation. In contrast to wall skin friction dependency, the wall heat transfer parameter shows a secondary dependence on the streamwise pressure gradient and the buoyancy force.**

## Nomenclature

$C$ = constant appearing in $U_e = Cx^m$, $= U_o/L_c^m$
$C_{fx}$ = local skin friction coefficient
$C_p$ = specific heat
$Fr$ = Froude number, $= U_e^3/U_o L_c g_x$
$f$ = nondimensional stream function of liquid flow
$g$ = nondimensional stream function of vapor flow
$h_{fg}$ = latent heat of vaporization
$h_x$ = local heat transfer coefficient
$Ja_L$ = Jakob number of liquid, $= C_{pL}(T_{sat} - T_\infty)/h_{fg}$
$Ja_v$ = Jakob number of vapor, $= C_{pv}(T_w - T_{sat})/h_{fg}$
$k$ = thermal conductivity of fluid
$L_c$ = characteristic length of the wedge
$m$ = pressure gradient parameter
$\dot{m}$ = mass flow rate of vapor per unit area
$Nu_x$ = local Nusselt number
$P$ = pressure
$Pr$ = Prandtl number
$q''w$ = local wall heat flux
$R$ = nondimensional density-viscosity product ratio, $= \rho_v\mu_v/\rho_L\mu_L$
$Re_{\delta v}$ = vapor film Reynolds number, $= \rho_v u_i \delta_v/\mu_v$
$Re_x$ = local liquid Reynolds number, $= \rho_L U_\infty x/\mu_L$
$r$ = density
$T$ = temperature
$T_{sat}$ = saturation temperature
$\mu$ = absolute viscosity
$T_w$ = wall temperature
$T_\infty$ = freestream liquid temperature
$\tau$ = shear stress
$U_e$ = liquid free stream velocity at the edge of liquid boundary layer
$U_0$ = reference velocity (taken as $U_e$ @ $\chi = L_c$)
$U_\infty$ = liquid upstream velocity (unaffected by wedge geometry)
$u$ = streamwise component of velocity
$u_i$ = interfacial (liquid-vapor interface) velocity
$v$ = vertical component of velocity
$x$ = streamwise coordinate
$y$ = normal coordinate
$\beta$ = pressure gradient parameter, $= 2m/(m + 1)$
$\delta_v$ = vapor film thickness
$\eta$ = nondimensional normal coordinate
$\eta_{v\delta}$, $\eta_{L\delta}$ = nondimensional vapor film thickness
$\lambda$ = nondimensional streamwise coordinate, $= 2\xi(\rho_L - \rho_v)/Fr\rho_v$
$\xi$ = nondimensional streamwise coordinate, $= (x/L_c)^{m+1}/(m + 1)$
$\psi$ = stream function

*Subscripts*
$v$ = vapor
$L$ = liquid

*Superscript*
$'$ = differentiation with respect to $\eta_L$ or $\eta_v$ as applicable

Received May 14, 1990; presented as Paper 90-1724 at the AIAA/ASME 5th Joint Thermophysics and Heat Transfer Conference, Seattle, WA, June 18–20, 1990; revision received Aug. 28, 1990; accepted for publication Aug. 29, 1990. This paper is declared a work of the U.S. Government and is not subject to copyright protection in the United States.

*Postdoctoral Fellow, Nuclear Technology and Engineering Division, Engineering and Society Analysis Group, M.S.K-557.
†Associate Professor, Department of Mechanical Engineering, P.O. Box 25000.
‡Staff Member, Nuclear Technology and Engineering Division, Engineering and Safety Analysis Group, M.S.K.-557.

## Introduction

THE influence of boiling on the drag of objects attracted the attention of a few investigators[1–7]: Cess and Sparrow,[2] Bradfield et al.,[1] and others[5,7] analyzed the forced convection film boiling flow in the context of reducing drag on objects. Another reason for this interest is that such information may be useful in analyzing the molten fuel relocation in postulated nuclear mishap scenarios.[4] In this study, subcooled forced convection film boiling analysis on a wedge geometry is performed to understand the effect of film boiling on skin friction drag and heat transfer. Wedge geometry is chosen so that a steamwise pressure gradient can be imposed

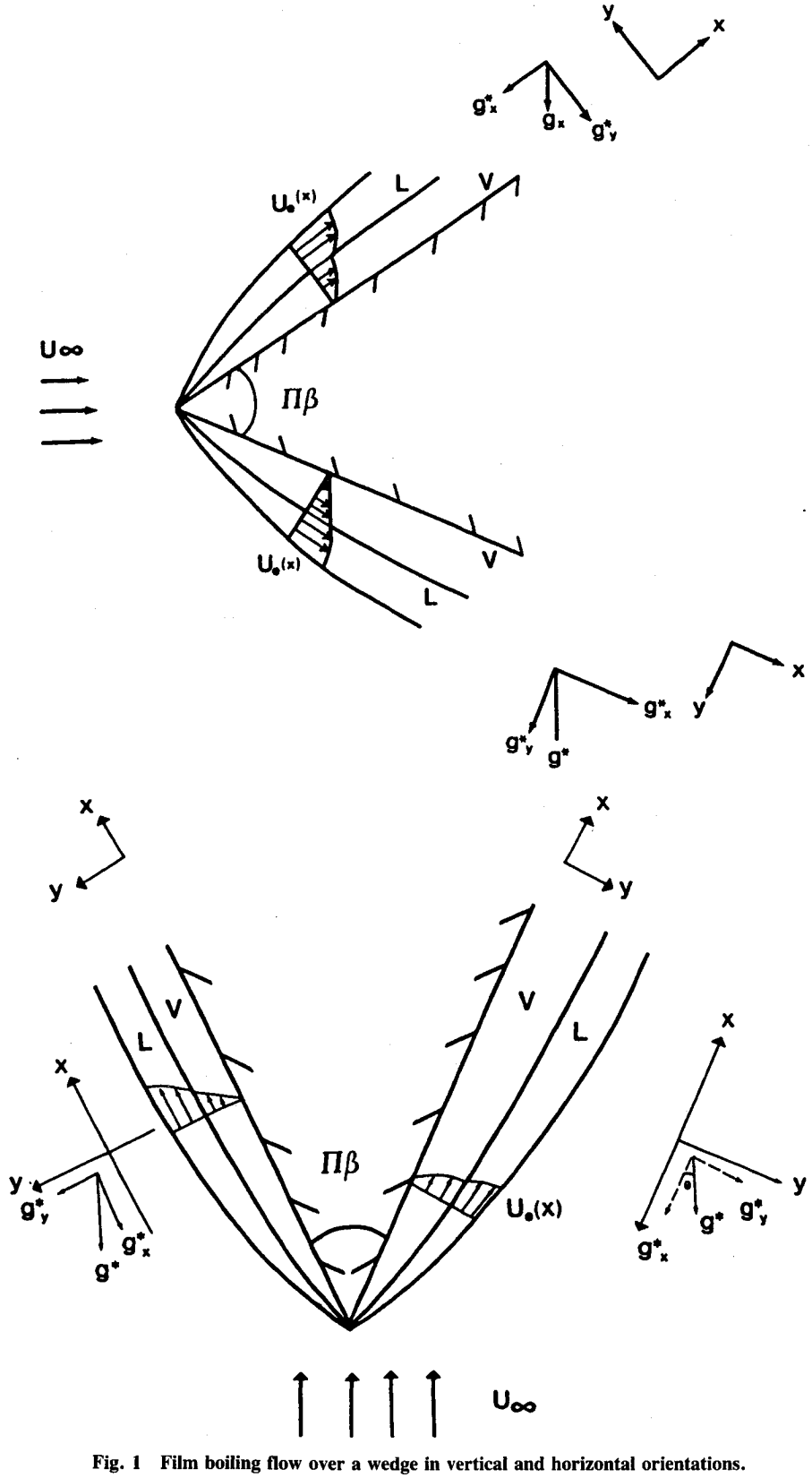


**Fig. 1 Film boiling flow over a wedge in vertical and horizontal orientations.**

on the flow, which is the case for a flow over any finite-thickness bodies such as a circular cylinder and sphere. The results of the wedge flow serve as a guide in understanding film boiling flow and heat transfer on cylindrical and spherical geometries, and these results may be used to devise approximate solutions.

Figure 1 shows a semi-infinite wedge in vertical and horizontal orientations; the orientation is important with respect to the buoyancy effects on the flow, as will be described later. If the temperature of the wedge is assumed to be sufficiently high to promote and maintain stable film boiling conditions, a thin vapor film forms adjacent to the wedge surface. Subcooled liquid flows on top of this vapor film. The two-phase boundary-layer concept, proposed by Cess and Sparrow,[2] is used to describe the vapor film and liquid flow.

None of the analyses[6-8] consider the influence of the streamwise buoyancy force on flow film boiling. For example, at atmospheric pressure for a water-steam system, the density

difference between the vapor and liquid is of the order of 1000 and the streamwise buoyancy force driving the vapor film over the wedge may be of the same order of magnitude as the other terms in the vapor flow momentum equation. Unless the wedge is very thin and lies in horizontal orientation (implying that the streamwise gravitational force component in the vapor flow momentum equation is negligible) or the Froude number is very large, the buoyancy force may have to be considered in the analysis. Consequently, the analyses[6–8] neglecting the effect of the buoyancy force may be valid only for horizontal wedges with a small included angle.[8] As to be demonstrated in this paper, consideration of the buoyancy force on the vapor flow reveals several new features of flow physics.

## Analysis

As discussed in the introduction, in a stable film boiling flow, a thin vapor film is assumed to form adjacent to the wedge surface and liquid flows on top of the vapor film. Several investigators (including current analysis) have modeled the thin vapor film flow and the liquid flow assuming a boundary-layer behavior.[1–3,5–8] It incorporates the following assumptions.

1) Steady, two-dimensional, incompressible and laminar flow is assumed in both phases.

2) Properties of both phases are estimated using the film temperature method.

3) Radiation from the solid surface is negligible.

4) The liquid-vapor interface is assumed to be smooth and at constant saturation temperature. Surface tension effects are neglected.

5) The liquid freestream velocity is unaffected by the presence of the vapor and liquid boundary layers.

The incompressibility assumption is best justified at low velocities ($U_\infty < 15$ ft/s),[1] and the laminar flow assumption in the vapor film requires $Re_{\delta_v} \leq 100$.[9] Assumption 2 is made on the basis of work reported in Reference 10. Assumption 3 and the smooth interface liquid-vapor assumption may be valid only in subcooled liquid conditions.[1,11,12] Thus, the current study is valid only under subcooled conditions. Nevertheless, saturation conditions are considered in the analysis to gain some idea regarding parametric trends. Away from the leading edge where the boundary-layer equations are applicable, the curvature of the liquid-vapor interface is less and, consequently, the surface tension effects may be unimportant.

Governing equations are derived for each phase and coupled at the liquid-vapor interface by the appropriate conservation equations.[3] Equations (1–16) are summarized in the following.

Vapor ($y < \delta_v$):

$$\frac{\partial u_v}{\partial x} + \frac{\partial v_v}{\partial y} = 0 \tag{1}$$

$$\rho_v\left(u_v \frac{\partial u_v}{\partial x} + v_v \frac{\partial u_v}{\partial y}\right) = \rho_L U_e \frac{dU_e}{dx} + \mu_v \frac{\partial^2 u_v}{\partial y^2} + (\rho_L - \rho_v)g_x \tag{2}$$

$$\frac{\partial p_v}{\partial y} \approx 0 \tag{3}$$

$$\rho_v C_{pv}\left(u_v \frac{\partial T_v}{\partial x} + v_v \frac{\partial T_v}{\partial y}\right) = k_v \frac{\partial^2 T_v}{\partial y^2} \tag{4}$$

Liquid ($y > \delta_v$):

$$\frac{\partial u_L}{\partial x} + \frac{\partial v_L}{\partial y} = 0 \tag{5}$$

$$\rho_L\left(u_L \frac{\partial u_L}{\partial x} + v_L \frac{\partial u_L}{\partial y}\right) = \rho_L U_e \frac{dU_e}{dx} + \mu_L \frac{\partial^2 u_L}{\partial y^2} \tag{6}$$

$$\frac{\partial p_L}{\partial y} \approx 0 \tag{7}$$

$$\rho_L C_{pL}\left(u_L \frac{\partial T_L}{\partial x} + v_L \frac{\partial T_L}{\partial y}\right) = k_L \frac{\partial^2 T_L}{\partial y^2} \tag{8}$$

Liquid-vapor interface ($y = \delta_v$):

$$u_v = u_L \tag{9}$$

$$\rho_v\left(u_v \frac{d\delta_v}{dx} - v_v\right) = \rho_L\left(u_L \frac{d\delta_v}{dx} - v_L\right) = \dot{m} \tag{10}$$

$$\mu_v \frac{\partial u_v}{\partial y} = \mu_L \frac{\partial u_L}{\partial y} \tag{11}$$

$$p_v = p_L \tag{12}$$

$$T_v = T_L = T_{sat} \tag{13}$$

$$-k_v \frac{\partial T_v}{\partial y} = -k_L \frac{\partial T_L}{\partial y} + \dot{m} h_{fg} \tag{14}$$

Boundary conditions ($y = 0$, $y \to \infty$):

$$\text{At } y = 0; \qquad u_v = v_v = 0, \qquad T_v = T_w \tag{15}$$

$$\text{As } y \to \infty; \qquad u_L \to U_e(x) = Cx^m, \qquad T_L \to T_\infty \tag{16}$$

where $C$ is a constant.

The liquid pressure gradient is first determined considering the velocity distribution [Eq. (16)] and the gravity effect in the inviscid liquid flow. Matching the pressures of liquid and vapor at the liquid-vapor interface [Eq. (12)] results in the appearance of the buoyancy force term and the freestream velocity gradient term in Eq. (2). Subsequently, the gravity effects are neglected relative to forced convection within the liquid boundary layer resulting in the form of Eq. (6).

For the vapor film and the liquid boundary layers, following Sparrow et al.[13] and Sparrow and Yu,[14] the following variables are introduced to analyze this nonsimilar two-phase boundary-layer flow:

$$\lambda = \frac{2\xi U_e L_e g_x(\rho_L - \rho_v)}{\rho_v U_e^3}$$

where

$$\xi = \frac{(x/L_e)^{m+1}}{m+1} \tag{17}$$

$$\eta_v = y\left(\frac{m+1}{2}\frac{U_e}{\nu_v x}\right)^{1/2}$$

$$\eta_L = y\left(\frac{m+1}{2}\frac{U_e}{\nu_L x}\right)^{1/2} \tag{18}$$

$$g(\lambda, \eta_v) = \frac{\psi_v}{[(2/m+1)\nu_v x U_e]^{1/2}}$$

$$f(\lambda, \eta_L) = \frac{\psi_L}{[(2/m+1)\nu_L x U_e]^{1/2}} \tag{19}$$

$$\theta_v = \frac{T_v - T_{sat}}{T_w - T_{sat}}, \qquad \theta_L = \frac{T_L - T_{sat}}{T_{sat} - T_\infty} \tag{20}$$

The variable $\lambda$ takes into account the influence of gravity and can be interpreted as follows

$$\lambda = \frac{2\xi}{Fr}\left(\frac{\rho_L}{\rho_v} - 1\right)$$

where

$$Fr = \frac{U_e^3}{U_0 L_c g_x} \tag{21}$$

Using the nondimensional variables used earlier, Eqs. (1–16) are transformed into Eqs. (22–32) as follows.

Vapor ($\eta_v < \eta_{v\delta}$):

$$g''' + gg'' + \beta\left(\frac{\rho_L}{\rho_v} - g'^2\right) + \lambda = \frac{2(1-2m)}{m+1}\lambda\left(g'\frac{\partial g'}{\partial\lambda} - g''\frac{\partial g}{\partial\lambda}\right) \tag{22}$$

$$\frac{1}{Pr_v}\theta_v'' + g\theta_v' = \frac{2(1-2m)}{m+1}\lambda\left(g'\frac{\partial\theta_v'}{\partial\lambda} - \theta_v'\frac{\partial g}{\partial\lambda}\right) \tag{23}$$

Liquid ($\eta_L > \eta_{L\delta}$):

$$f''' + ff'' + \beta(1 - f'^2) = \frac{2(1-2m)}{m+1}\lambda\left(f'\frac{\partial f'}{\partial\lambda} - f''\frac{\partial f}{\partial\lambda}\right) \tag{24}$$

$$\frac{1}{Pr_L}\theta_L'' + f\theta_L' = \frac{2(1-2m)}{m+1}\lambda\left(f'\frac{\partial\theta_L'}{\partial\lambda} - \theta_L'\frac{\partial f}{\partial\lambda}\right) \tag{25}$$

Liquid-vapor interface ($\eta_v = \eta_{v\delta}$ or $\eta_L = \eta_{L\delta}$):

$$g' = f' \tag{26}$$

$$g + \frac{2(1-2m)}{m+1}\lambda\frac{\partial g}{\partial\lambda} = R^{-1/2}\left(f + 2\lambda\left(\frac{1-2m}{m+1}\right)\frac{\partial f}{\partial\lambda}\right) \tag{27}$$

$$g'' = R^{-1/2} f'' \tag{28}$$

$$\theta_v = 0, \qquad \theta_L = 1 \tag{29}$$

$$Ja_v = \frac{Ja_L R^{-1/2} Pr_v}{Pr_L}\frac{\theta_L'}{\theta_v'} - \frac{Pr_v}{\theta_v'}\left(g + 2\lambda\frac{(1-2m)}{m+1}\frac{\partial g}{\partial\lambda}\right) \tag{30}$$

Boundary conditions ($\eta_v = 0$, $\eta_L \to \infty$):

At $\eta_v = 0$; $\quad g' = 0$,

$$g + 2\left(\frac{1-2m}{m+1}\right)\lambda\frac{\partial g}{\partial\lambda} = 0, \qquad \theta_v = 1 \tag{31}$$

As $\eta_L \to \infty$; $\quad f' \to 1, \quad \theta_L \to 1$ (32)

To solve this system of equations, the local similarity method proposed by Sparrow et al.[13] and Sparrow and Yu[14] is used in the current analysis. Under this approximation, the derivatives with respect to

$$\lambda\left[\frac{\partial g}{\partial\lambda}, \frac{\partial}{\partial\lambda}\left(\frac{\partial g}{\partial\eta_v}\right), \frac{\partial\theta_v}{\partial\lambda}, \frac{\partial}{\partial\lambda}\left(\frac{\partial\theta_v}{\partial\eta_v}\right), \frac{\partial f}{\partial\lambda}, \frac{\partial}{\partial\lambda}\left(\frac{\partial f}{\partial\eta_L}\right), \frac{\partial\theta_L}{\partial\lambda}, \frac{\partial}{\partial\lambda}\left(\frac{\partial\theta_L}{\partial\eta_L}\right)\right]$$

are postulated to be small and drop out of Eqs. (22–32) when $\lambda$ is large; at the other limit also, when $\lambda$ is small, the terms of nonsimilar nature are eliminated. It is difficult to estimate a priori the extent of error committed by this approximation, and this, in fact, is the major pitfall of the local similarity approximation.

With the local similarity approximation, Eqs. (22–32) reduce to the following form.

Vapor ($\eta_v < \eta_{v\delta}$):

$$g''' + gg'' + \beta\left(\frac{\rho_L}{\rho_v} - g'^2\right) + \frac{2\xi}{Fr}\left(\frac{\rho_L}{\rho_v} - 1\right) \approx 0 \tag{33}$$

$$\theta_v'' + Pr_v\, g\theta_v' \approx 0 \tag{34}$$

Liquid ($\eta_L > \eta_{L\delta}$):

$$f''' + ff'' + \beta(1 - f'^2) \approx 0 \tag{35}$$

$$\theta_L'' + Pr_L f\theta_L' \approx 0 \tag{36}$$

Liquid-vapor interface ($\eta_v = \eta_{v\delta}$ or $\eta_L = \eta_{L\delta}$):

$$g' \approx f' \tag{37}$$

$$g \approx R^{-1/2} f \tag{38}$$

$$g'' \approx R^{-1/2} f'' \tag{39}$$

$$\theta_v = 0, \qquad \theta_L = 1 \tag{40}$$

$$Ja_v = \frac{Ja_L R^{-1/2} Pr_v}{Pr_L}\frac{\theta_L'}{\theta_v'} - \frac{Pr_v}{\theta_v'}g \tag{41}$$

Boundary conditions ($\eta_v = 0$, $\eta_L \to \infty$):

At $\eta_v = 0$; $\quad g' = 0, \quad g = 0, \quad \theta_v = 1$ (42)

As $\eta_L \to \infty$; $\quad f' \to 1, \quad \theta_L \to 1$ (43)

Equations (33–43) are solved (described later) for velocity and temperature profiles, and the results are displayed via skin friction coefficient and Nusselt number, namely,

$$C_{fx} = \frac{\mu_v\left\langle\frac{\partial u_v}{\partial y}\right\rangle_{y=0}}{\frac{1}{2}\rho_L U_e^2} \Rightarrow \frac{C_{fx}\sqrt{Re_x}}{2} = R^{1/2}\left(\frac{m+1}{2}\right)^{1/2} g''(0) \tag{44}$$

$$Nu_x = \frac{hx}{k_v} = \frac{-(\partial T_v/\partial x)x}{(T_w - T_{sat})} \Rightarrow \frac{Nu_x}{\sqrt{Re_x}}\left(\frac{\mu_v}{\mu_L}\right) = -R^{1/2}\left(\frac{m+1}{2}\right)^{1/2}\theta_v'(0) \tag{45}$$

**Table 1 Grid sizes**

| $\eta_v$ | $\Delta\eta_v$ |
|---|---|
| 0.001–0.005 | 0.0001 |
| 0.005–0.5 | 0.001 |
| 0.5–1.0 | 0.005 |
| 1.0–5.0 | 0.01 |
| $\Delta\eta_L$ | = 0.03 |

## Solution Methodology

Of the eight explicitly prescribable parameters in the governing equations [Eqs. (33–45)], seven are $2\xi/Fr$ (buoyancy force parameter), $\beta = 2m/(m+1)$ (pressure gradient parameter), $\rho_L/\rho_v$ (density ratio parameter), $R = (\rho_v\mu_v)/(\rho_L\mu_L)$ (density-viscosity product ratio parameter), $Pr_v$ (vapor Prandtl number), $Pr_L$ (liquid Prandtl number), and $Ja_L$ (liquid subcooling parameter, namely, liquid Jakob number). For the choice of the eighth parameter, it is to be noted that $\eta_{v\delta}$ (nondimensional vapor film thickness) and $Ja_v$ (wall superheat parameter, namely, vapor Jakob number) are related implicitly to each other by Eq. (41). As done earlier,[8,15] the nondimensional vapor film thickness $\eta_{v\delta}$ is chosen to be the eighth parameter, and the corresponding wall superheat parameter $Ja_v$ is calculated from Eq. (41) as a final step in the solution of the governing equations [Eqs. (33–45)].

A fourth-order Runge-Kutta method with a shooting technique [to find the missing wall shear, $g''(0)$] is used to solve the momentum equations of the vapor and liquid flow [Eqs. (33) and (35) along with the conditions Eqs. (37–39), (42), and (43)] for the vapor and liquid velocity profiles. Using these velocity profiles, the energy equations [Eqs. (34) and (36)] along with the conditions [Eqs. (40), (42), and (43)] of the vapor and liquid phases are solved in an implicit finite difference form.

Using the temperature profiles, the temperature gradient of vapor at the wall $\theta_v'(0)$, the temperature of the liquid at the liquid-vapor interface $\theta_L'(\eta_{v\delta})$, and the temperature gradient of the vapor at the liquid-vapor interface $\theta_v'(\eta_{v\delta})$ is calculated by second-order difference approximations. The velocity and temperature profiles in combination with the

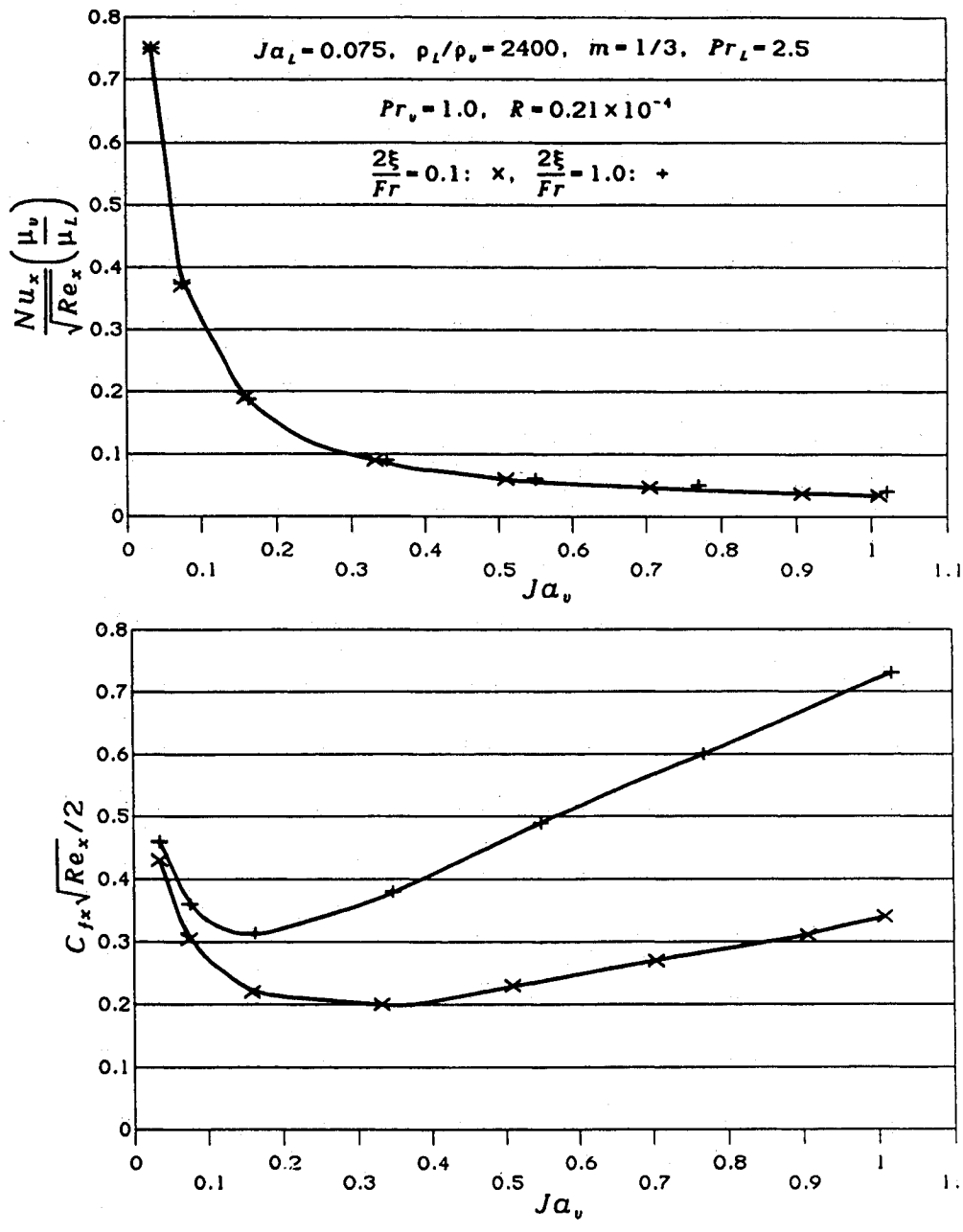


**Fig. 2 Effect of the streamwise buoyancy force (favorable) parameter, $2/Fr$.**

gradients then are used to evaluate nondimensional skin friction, heat transfer, and wall superheat parameters from Eqs. (44), (45), and (41), respectively.

During this analysis, the effect of approximating infinity in the liquid boundary layer by a finite distance, the tolerance limit on satisfying the boundary conditions at the outer edge of the liquid boundary layer, and the grid spacing in the vapor film and the liquid layer were examined for various conditions. These tests and random checking of the results during the course of computations were used to assess the numerical uncertainty of the results. Accuracy was satisfied up to the third decimal place in most of these calculations. Based on these tests, the freestream boundary conditions at infinity were satisfied at a finite dimension, $\eta_{L,\max} = 6$, with an accuracy of $\varepsilon = 10^{-4}$. The combination of grid sizes used in this study, as used earlier,[8] is given in Table 1.

Because of the coupled nonlinearity of the governing differential equations, the fourth-order Runge-Kutta method along with the shooting technique used in the solution methodology are sensitive to the starting input value of $g''(0)$. Choosing a low value of $\eta_{v\delta}$ initially and increasing it steadily would facilitate easier guessing of the starting input value of $g''(0)$. After the initial input value of $g''(0)$ is given to start the Runge-Kutta procedure, convergence is obtained by using a bisection method to refine the wall shear $g''(0)$. If the flow is accelerated strongly (i.e., at large parametric values of the buoyancy force parameter $2\xi/Fr$, say 100), the tolerance limit of satisfying the freestream boundary condition is increased from $10^{-4}$ to $10^{-3}$ or $10^{-2}$.

## Discussion of Results

The current numerical procedure initially was verified by reproducing the results of Ito and Nishikawa[15] and Nakayama.[7] A water-steam system at atmospheric pressure with subcoolings from 20 to 100°C and encompassing wall superheats of 100–600°C is considered in this study. Fluid properties were evaluated at the respective film temperatures of the vapor and liquid. Because the vapor Prandtl number (≈1) varies negligibly in the above wall superheat range, a constant value of unity was assigned.

It is to be noted that, on a vertical wedge with an upward flow (Fig. 1), the streamwise component of buoyancy force acting on the vapor film always aids the vapor flow on both surfaces of the wedge. However, on a horizontal wedge (Fig. 1), it is favorable to the flow on the upper surface and opposes the flow on the lower surface. Thus, the current analysis with

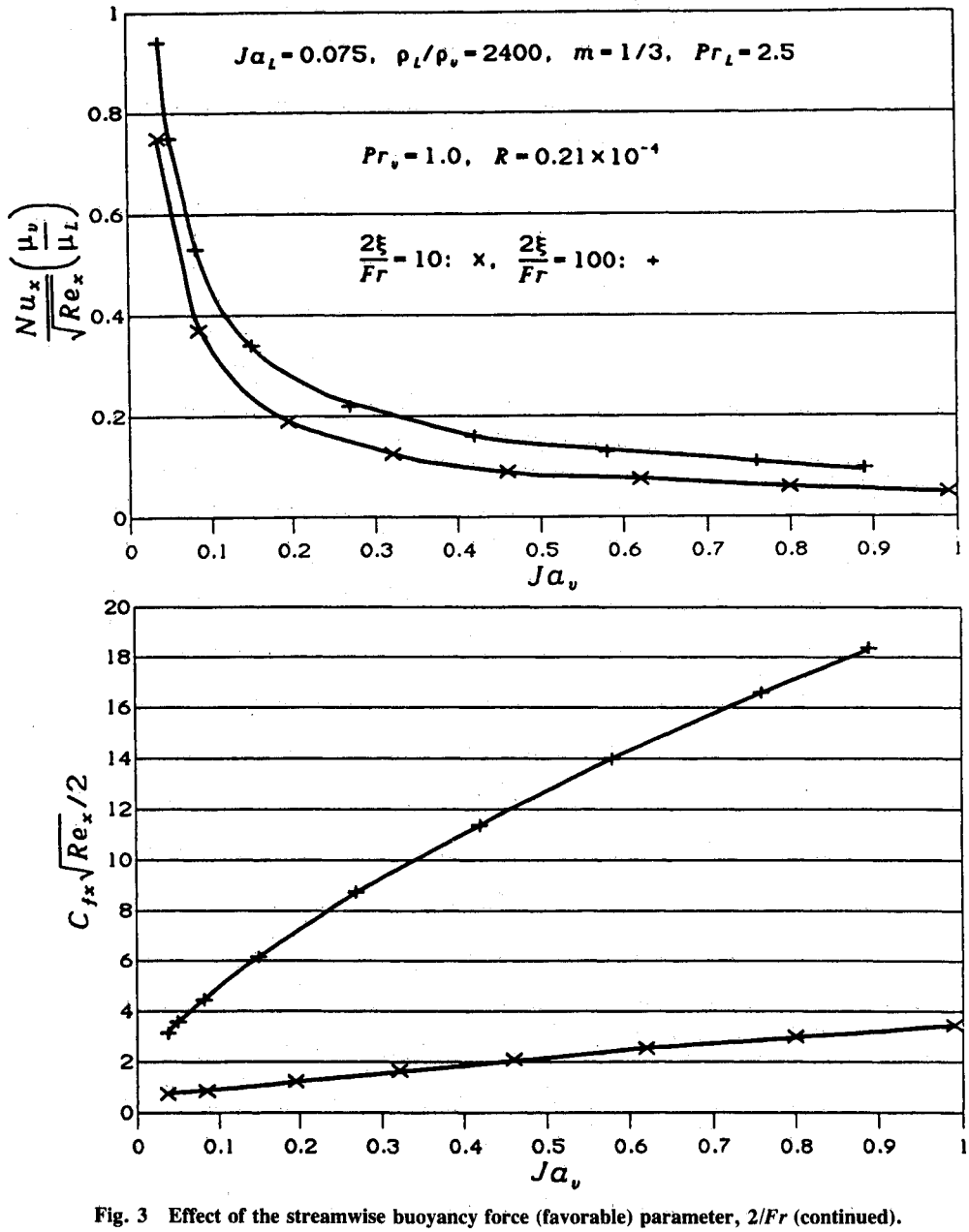


**Fig. 3 Effect of the streamwise buoyancy force (favorable) parameter, $2/Fr$ (continued).**

**Table 2 Calculations illustrating Cousette flow hypothesis**

| $Ja_v$ | $g''(0)$ | $\eta_{v\delta}$ | $g_i'$ | $\frac{g_i'}{\eta_{v\delta}}$ | $\frac{\eta_{v\delta}}{2}\frac{2m}{m+1}\frac{\rho_L}{\rho_v}$ | $\frac{\eta_{v\delta}}{2}\frac{2\xi}{Fr}\left[\frac{\rho_L}{\rho_v}-1\right]$ |
|---|---|---|---|---|---|---|
| | | | | $\frac{2\xi}{Fr}=0.1$ | | |
| 0.159 | 58.8 | 0.02 | 0.888 | 44.4 | 12 | 2.4 |
| 0.333 | 54.05 | 0.04 | 1.01 | 25.25 | 24 | 4.8 |
| 0.705 | 72 | 0.08 | 1.152 | 14.4 | 48 | 9.6 |
| | | | | $\frac{2\xi}{Fr}=10.0$ | | |
| 0.195 | 330.4 | 0.02 | 1.57 | 78.50 | 12 | 239.9 |
| 0.322 | 433.23 | 0.03 | 1.96 | 65.33 | 18 | 359.9 |
| 0.62 | 803.87 | 0.06 | 2.89 | 48.17 | 36 | 719.7 |

a favorable streamwise component of buoyancy force is equally valid for the vertical wedge with an upward flow and the upper surface of a horizontal wedge.

A low value of the buoyancy force parameter, $2\xi/Fr$, implies that either the nondimensional streamwise length $\xi$ is small or the local Froude number is large (meaning domination of velocity effects over gravity effects). As $2\xi/Fr$ increases from 0.1 and 100 (which implies a domination of the favorable buoyancy force driving the vapor flow), the local skin friction parameter, $C_{fx}\sqrt{Re_x}/2$, and the local heat transfer parameter

$$\frac{Nu_x}{\sqrt{Re_x}}\left(\frac{\mu_v}{\mu_L}\right)$$

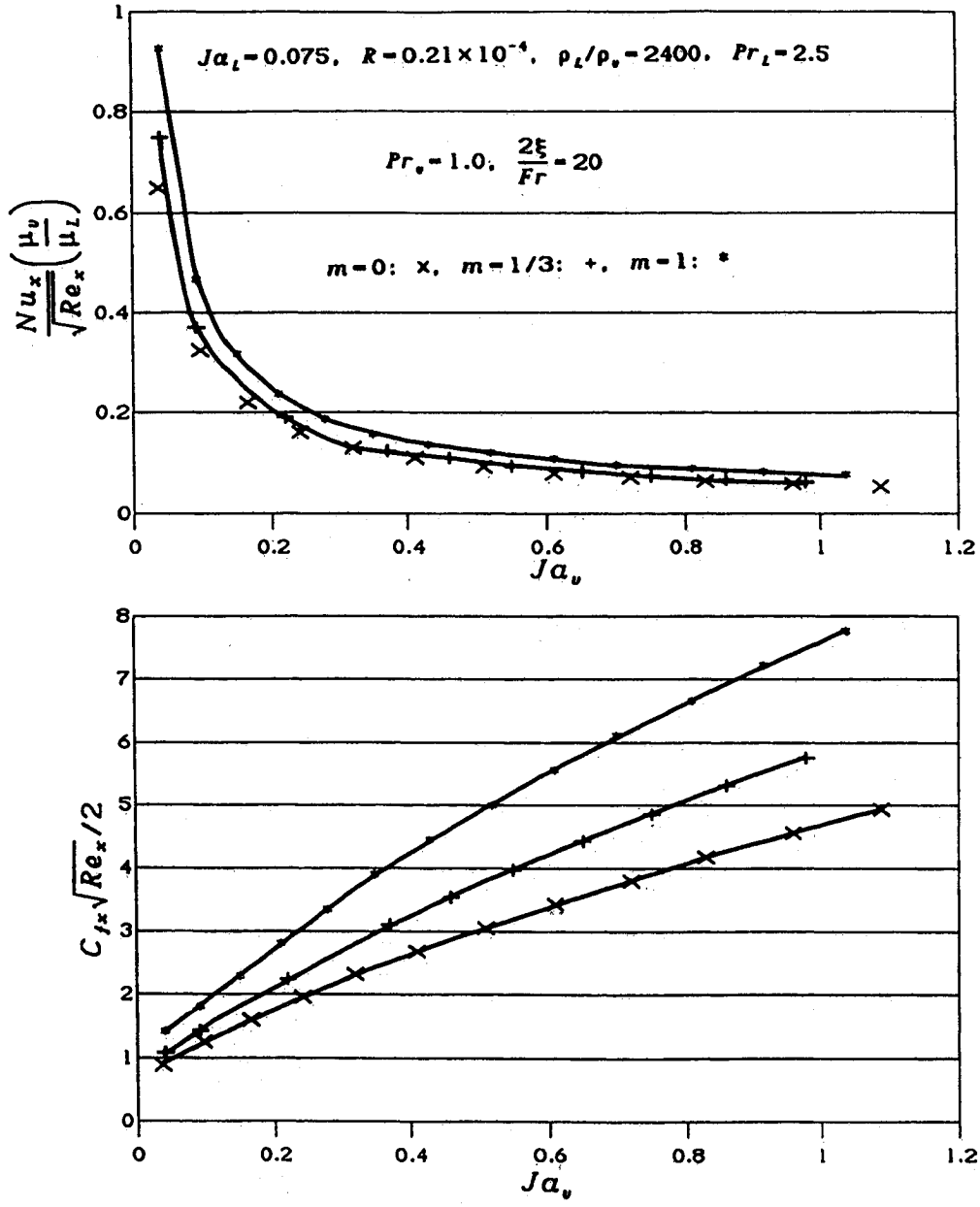


Fig. 4 Influence of the pressure gradient parameter $m$.

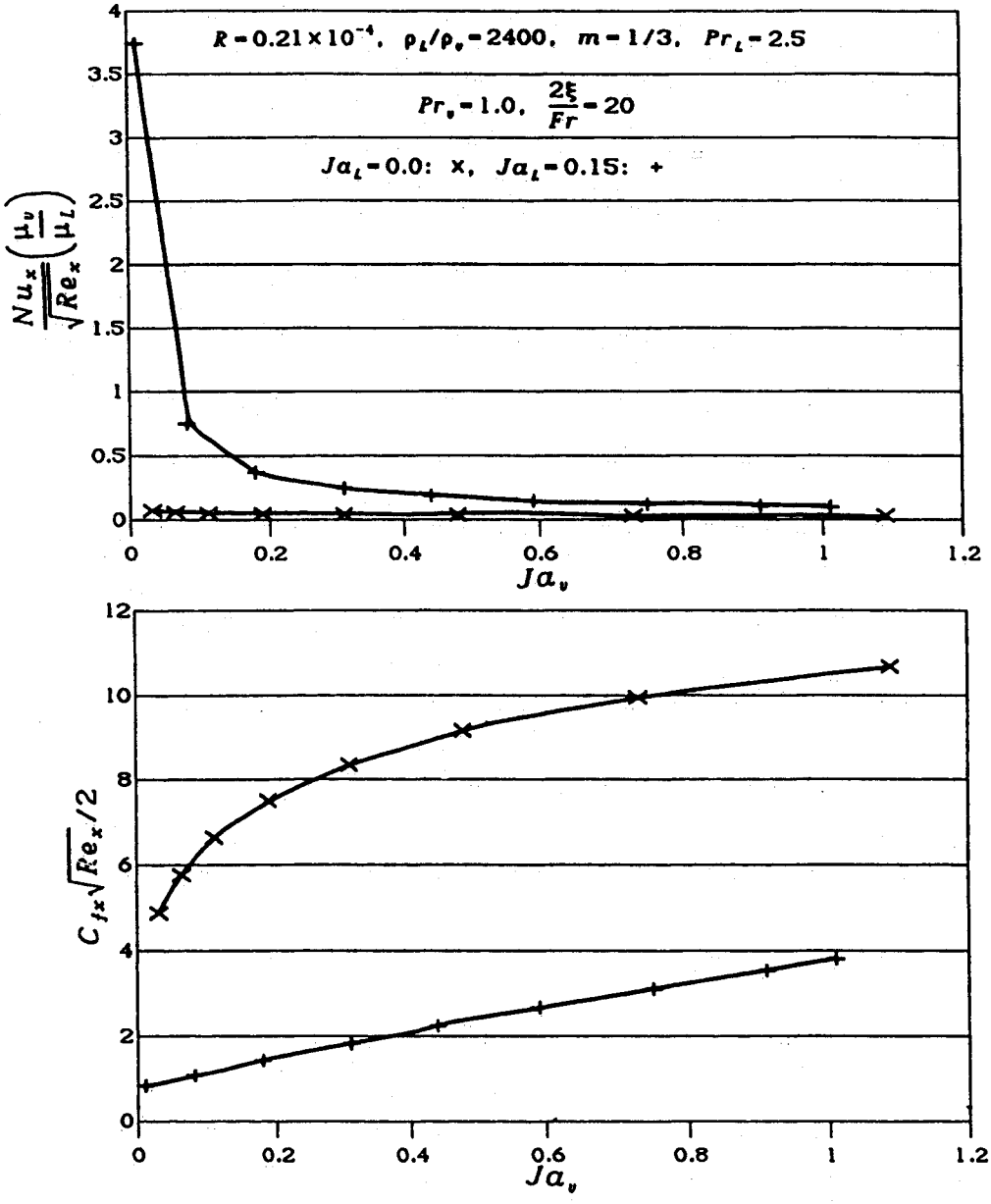


**Fig. 5 Influence of liquid subcooling parameter $Ja_L$.**

also increase (see Figs. 2 and 3). This trend is understandable because favorable buoyancy force accelerates the vapor film flow, resulting in higher vapor flow velocities, which should cause an increase in local wall skin friction and heat transfer.

At low values of the buoyancy force parameter, $2\xi/Fr = 0.1, 1$, the skin friction parameter, $C_{fx}\sqrt{Re_x}/2$, initially decreases, reaches a minimum, and starts increasing with increasing wall superheat parameter $Ja_v$. It can be observed that the local skin friction parameter, $C_{fx}\sqrt{Re_x}/2$, at higher values of the buoyancy force parameter, $2\xi/Fr = 10, 100$, exhibits a monotonic increase with an increase in the wall superheat parameter $Ja_v$.

The trends exhibited by the skin friction parameter can be explained (on a first-order basis) by approximating the vapor film flow locally as a Couette flow. The wall shear on the wedge can be written as

$$\tau_w = \mu_v \left\langle \frac{\partial u_v}{\partial y} \right\rangle_{y=0} \cong \mu_v \frac{u_{vi}}{\delta_v} + \frac{\delta_v}{2}\left\{\rho_L U_e \frac{dU_e}{dx} + (\rho_L - \rho_v)g_x\right\} \tag{46}$$

In the nondimensional variables of the current analysis

$$g''(0) \cong \frac{g_i'}{\eta_{v\delta}} + \frac{\eta_{v\delta}}{2}\frac{2m\rho_L}{(m+1)\rho_v} + \frac{\eta_{v\delta}}{2}\frac{2\xi}{Fr}\left(\frac{\rho_L}{\rho_v} - 1\right) \tag{47}$$

In the Eq. (47), $g''(0)$ comprises the viscous shear contribution (without the effect of pressure gradient, for example, a flat-plate film boiling flow) of the vapor film [first term on the right side of Eq. (47)], the influence of the external streamwise pressure gradient on the flow (second term), and the effect of the local streamwise component of buoyancy on the vapor film (third term). When the buoyancy force driving the vapor film is low, the skin friction characteristics are dominated by the first term at low wall superheats and by the second term at higher wall superheats. Predictions in Table 2 (calculated by using numerically obtained values of $g_i'$, $\eta_{v\delta}$) at low values of $2\xi/Fr$ (say, 0.1) illustrate this hypothesis very clearly. Thus, the turn-around behavior of the local skin friction parameter (which initially decreases, reaches a minimum, and increases) with increased heating of the wedge (i.e., increasing $Ja_v$) is a result of the domination of the streamwise pressure gradient and the buoyancy force driving the flow at higher wall superheats. At a higher value of $2\xi/Fr$ (say 100), predictions in Table 2 show that the skin friction behavior is dominated by the buoyancy force term in Eq. (47). Thus, the

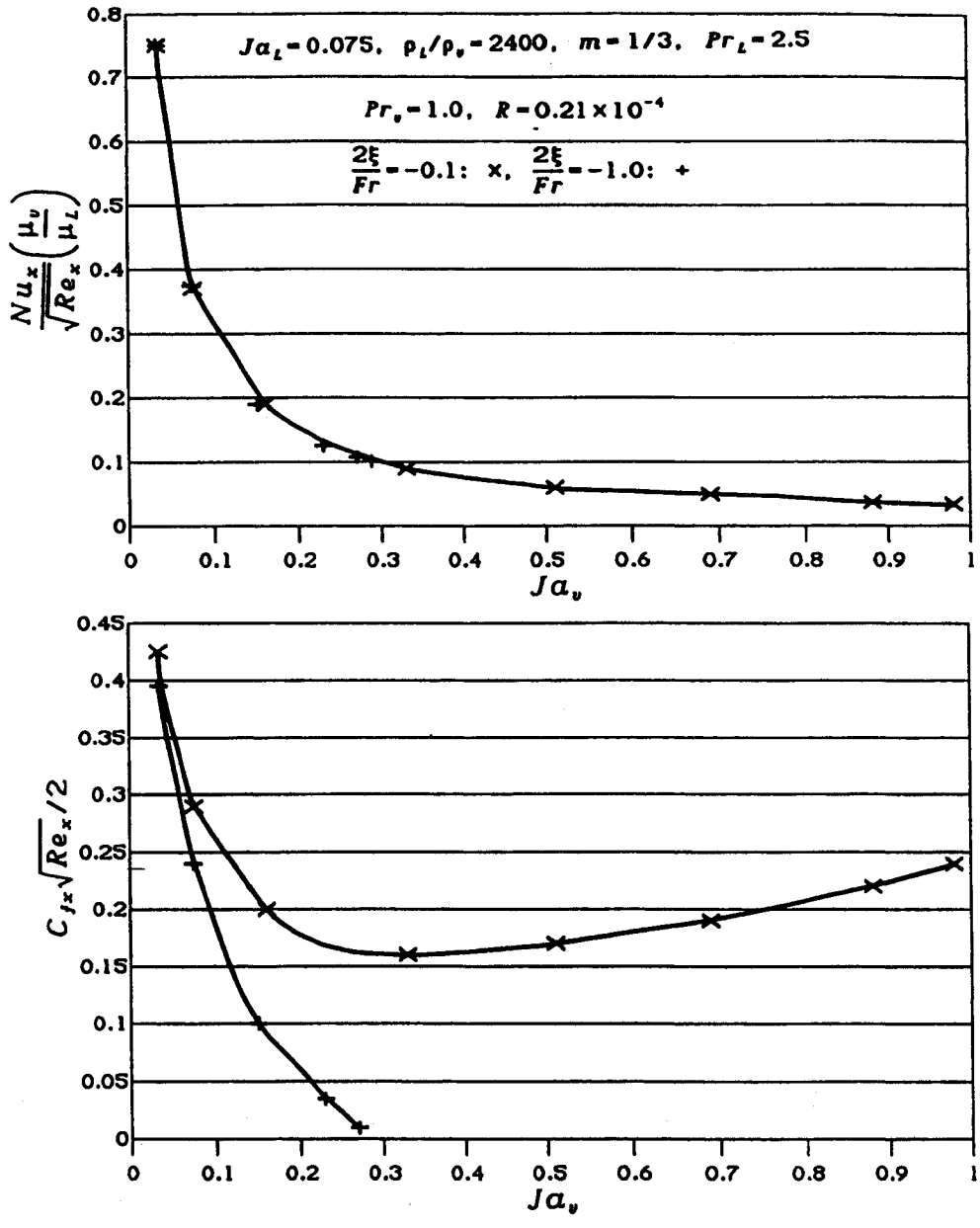


**Fig. 6 Opposing streamwise buoyancy force parameter effect, $2/Fr$.**

increasing trend of the local skin friction parameter with increased heating of the wedge (as observed in Fig. 4) is due to the domination of the streamwise buoyancy force term in Eq. (44). Figures 3 and 4 also show that the increase in the buoyancy force parameter causes the local wall heat transfer parameter

$$\frac{Nu_x}{\sqrt{Re_x}}\left(\frac{\mu_v}{\mu_L}\right)$$

to increase; however, the increase is not as large as the skin friction parameter.

Figure 4 shows that higher values of the pressure gradient parameter $\beta$ improves the local wall heat transfer and wall skin friction. The density ratio parameter $\rho_L/\rho_v$ should qualitatively exert the same influence as the favorable buoyancy force parameter $2\xi/Fr$ [see Eqs. (33) and (47)] because an increase in these parametric values signifies the acceleration of the film boiling flow leading to increased wall skin friction and heat transfer. To conserve space, figures illustrating the effect of the density ratio parameter $\rho_L/\rho_v$ on local skin friction and wall heat transfer are not shown. Although the wall heat transfer parameter

$$\frac{Nu_x}{\sqrt{Re_x}}\left(\frac{\mu_v}{\mu_L}\right)$$

shows an increase as the density ratio parameter increases, this improvement is marginal.

Figure 5 shows the influence of the liquid subcooling parameter $Ja_L$. With increased liquid subcooling, the local wall heat transfer parameter increases (signifying an increase in the local wall heat transfer coefficient). This is to be expected because $h \approx k_v/\delta_v$ and subcooling the liquid will decrease the vapor film thickness $\delta_v$. Subcooling the liquid (at the parametric values shown in the figure) decreases the wall skin friction parameter. For this buoyancy-dominated flow, $2\xi/Fr = 20$, similar to the trends as shown earlier for $2\xi/Fr = 100$ in Table 2, the buoyancy force term in Eq. (47) dominates the characteristics of the wall skin friction, and the influence of the other two terms in Eq. (47) is minor. The contribution of the buoyancy force term in Eq. (47) is linearly proportional to the vapor film thickness. Any decrease in vapor film thick-

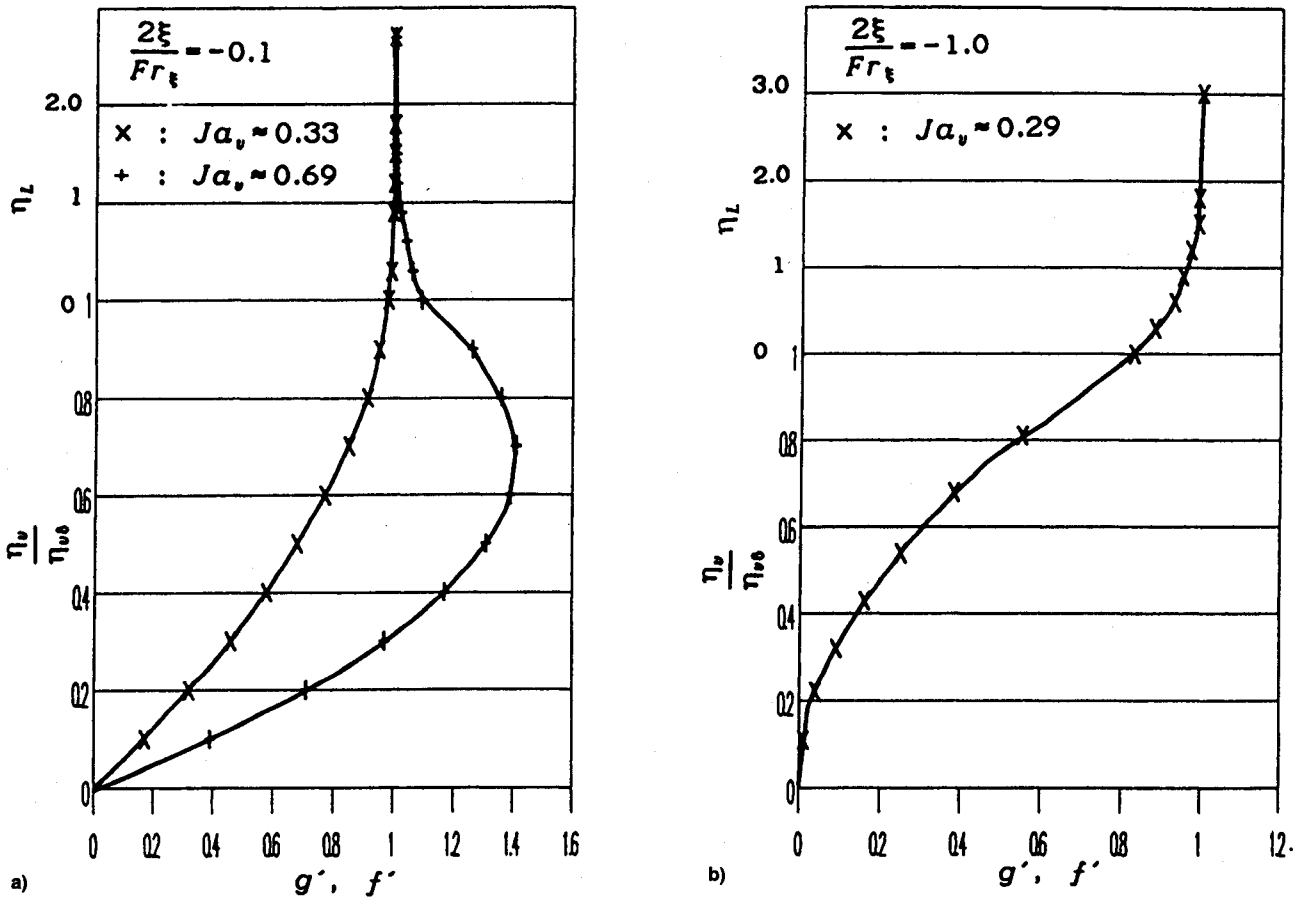


**Fig. 7 Velocity profiles as influenced by the adverse buoyancy force parameter $2/Fr$.**

ness as a result of increased liquid subcooling will reduce the local wall skin friction, as shown in Fig. 5.

The influence of the density-viscosity ratio parameter $R$ and the liquid Prandtl number $Pr_L$ are not shown in order to conserve space. For the water-steam system under consideration, the density-viscosity ratio parameter $R$ varies from $0.155 \times 10^{-4}$ to $0.272 \times 10^{-4}$ and the liquid Prandtl number varies from 1.75 to 3.0. The density- viscosity ratio parameter affects the local wall heat transfer predictions marginally in the parametric range considered. An increase in the liquid Prandtl number translates the skin friction and heat transfer curves toward lower wall superheats.

On the bottom surface of the horizontal wedge, the streamwise component of buoyancy force acting on the vapor film is adverse (Fig. 1); this effect is simulated by the negative values given to the buoyancy force parameter $2\xi/Fr$. This opposing buoyancy force slows down the vapor film, and the skin friction at the wall reduces (Figs. 6 and 7). If the opposing buoyancy force is large enough, the vapor film may stagnate and separate. A typical velocity profile of the vapor film close to separation is illustrated in Fig. 7b. The effect of the opposing buoyancy force parameter is marginal in wall heat transfer predictions (Fig. 6). Comparisons with the experimental data at this time could not be made because of lack of such information. Pending experimental comparisons, these results should be viewed with caution.

## Conclusions

Subcooled laminar forced convection film boiling flow on a wedge is analyzed, considering the streamwise pressure gradient and the buoyancy force acting on the vapor film. The major observations for a water-stream system at atmospheric pressure are the following:

1) The skin friction on a wedge in a film boiling flow may increase beyond the single-phase (all liquid) flow level. This feature is attributed to the consideration of the streamwise buoyancy force and the pressure gradient driving the vapor flow.

2) A turn-around behavior of the wall skin friction parameter with increased heating of the wedge (as demonstrated by earlier studies)[6,8] is possible only when the buoyancy force parameter driving the vapor film is low.

3) On the lower surface of a horizontally aligned wedge in a film boiling flow, the buoyancy force on vapor film acts adversely to the flow direction demonstrating a vapor flow separatin.

4) Wall heat transfer predictions, as opposed to skin friction predictions, demonstrated a secondary dependence on the buoyancy force parameter.

## References

[1]Bradfield, W. S., Barkdoll, R. O., and Bryne, J. T., "Some Effects of Boiling on Hydrodynamic Drag," *International Journal of Heat and Mass Transfer*, Vol. 5, No. 7, 1962, pp. 615–622.

[2]Cess, R. D., and Sparrow, E. M., "Film Boiling in Forced Convection Boundary-Layer Flow," *Journal of Heat Transfer*, Vol. 84, No. 3, 1961, pp. 370–376.

[3]Chappidi, P. R., "Drag Characteristics of Objects in Two-Phase Boiling Flows," Ph.D. Dissertation, University of Central Florida, Orlando, FL, Aug. 1989.

[4]Cho, D. H., and Lambert, G. A., "Effect of Boiling on Particle Drag," *Nuclear Engineering and Design*, Vol. 108, No. 3, 1988, pp. 523–524.

[5]Gay, A., "Film Boiling Heat Transfer and Drag Reduction," Convair Aerospace Division Report, GDCA-DDB-71-001, San Diego, CA, April 1971.

[6]Walsh, S. K., and Wilson, S. D. R., "Boundary-Layer Flow in Forced-Convection Film Boiling on a Wedge," *International Journal of Heat and Mass Transfer*, Vol. 22, No. 4, 1979, pp. 569–576.

[7]Nakayama, A., "Subcooled Forced Convection Film Boiling in

the Presence of a Pressure Gradient," *AIAA Journal*, Vol. 24, No. 2, 1986, pp. 230–236.

[8]Chappidi, P. R., and Gunnerson, F. S., "A Numerical Study of the Skin Friction and Heat Transfer Characteristics of a Wedge in Film Boiling Flow," *Proceedings of the 1988 National Heat Transfer Conference*, edited by H. R. Jacobs, ASME, New York, Houston, TX, Vol. 2, 1988, 475–486.

[9]Hsu, Y. Y., and Westwater, J. W., "Approximate Theory for Film Boiling on Vertical Surfaces," *Chemical Engineering Progress Symposium Series*, Vol. 56, No. 30, 1960, pp. 15–24.

[10]Bromley, L. A., Leroy, N. R., and Robbers, J. A., "Heat Transfer in Forced Convection Film Boiling," *Industrial and Engineering Chemistry*, Vol. 45, No. 12, 1953, pp. 2639–2646.

[11]Stevens, J. W., and Witte, L. C., "Destabilization of Vapor Film Flow Around Spheres," *International Journal of Heat and Mass Transfer*, Vol. 16, No. 3, 1973, pp. 669–678.

[12]Chappidi, P. R., Pasamehmetoglu, K. O., and Gunnerson, F. S., "The Influence of Surface Radiation on Forced Convection Film Boiling," Presented at *International Symposium on Gas-Liquid Two-Phase Flows, ASME Winter Annual Meeting*, Dallas, Texas, November 25–30, 1990.

[13]Sparrow, E. M., Quack, H., and Boerner, C. J., "Local Non-similarity Boundary-Layer Solutons," *AIAA Journal*, Vol. 8, No. 11, 1970, pp. 1936–1942.

[14]Sparrow, E. S., and Yu, H. S., "Local Non-Similarity Thermal Boundary-Layer Solutions," *Journal of Heat Transfer*, Vol. 92, No. 4, 1971, pp. 328–334.

[15]Ito, T., and Nishikawa, K., "Two-Phase Boundary-Layer Treatment of Forced-Convection Film Boiling," *International Journal of Heat and Mass Transfer*, Vol. 9, No. 2, 1966, pp. 117–130.